

Hydrothermal synthesis of zeolites from natural stellerite^①

LI Yan(李 阳), WANG Xin(汪 信), DONG Yuan-cai(董元彩), ZHU Jun-wu(朱俊武)
(Materials Chemistry Lab, Nanjing University of Science and Technology, Nanjing 210094, China)

[Abstract] Y and P zeolites were synthesized hydrothermally from natural stellerite under different conditions and were characterized via XRD and FT-IR. The results show that the higher crystallinity of Y zeolite can be obtained in hydrothermal system with low alkalinity, low $\text{Ca}^{2+}/\text{Na}^+$ ratio, and high $\text{SiO}_2/\text{Al}_2\text{O}_3$ ratio. The lattice space of the samples decreases as crystallization time increases. P Zeolite is prompted under condition of higher alkalinity and higher $\text{Ca}^{2+}/\text{Na}^+$ ratio. The intensity and number of bands in the range of $400\text{ cm}^{-1} \sim 900\text{ cm}^{-1}$ increases with reaction time. Bands at 680 cm^{-1} , 760 cm^{-1} and 860 cm^{-1} corresponding to Y zeolite appear during the crystallization stage. Most of these bands shift to higher wavenumbers when $\text{SiO}_2/\text{Al}_2\text{O}_3$ ratio increases generally. In the hydrothermal system with reverse condition above, bands at 600 cm^{-1} , $420\text{ cm}^{-1} \sim 470\text{ cm}^{-1}$ hardly change as the crystallization time increases and the main crystal phase of P zeolite is obtained.

[Key words] Y zeolite; P zeolite; stellerite; crystallinity; hydrothermal synthesis

[CLC number] P 426. 2

[Document code] A

1 INTRODUCTION

Zeolites are a family of hydrated aluminosilicate minerals which contain alkali and alkaline earth metal cations. They have a framework structure with interconnected cavities occupied by positively charged ions and water molecules. A favourable combination of physico-chemical properties is achieved by this particular structure. Zeolites are highly rated in their molecular sieving, adsorbing, catalytic and ion exchanging functions. They are used by the chemical industry as fertilizer, detergent builders, drying reagents for gases and liquids, selective molecular adsorbents for pollution abatement^[1~4], etc. As this has recently led to a steep increase in demand of these products, it is obvious that zeolites synthesized from low-cost natural silica-aluminate sources is becoming increasingly interesting in the fields of chemical industries and daily application. Zeolites are usually obtained synthetically by hydrothermal growth in an aqueous (alkaline) reactant mixture. By this day, the waste solid and natural minerals rich in SiO_2 and Al_2O_3 , such as flyash, tuff, pumice, kaolinite, etc., have been used as starting products for hydrothermal synthesis of zeolites^[5~7]. Regarding both aspects of efficient application of natural resources and economic factor for synthesis of zeolites, for the first time, the stellerite, a natural mineral resources located in the south of China, was taken as the starting materials of zeolites in our research. Y and P Zeolites were successfully synthesized from stellerite under hydrothermal condition. The phase transformation and zeolite

crystallinity were investigated via X-ray powder diffraction and IR spectrum measurements.

2 EXPERIMENTAL

The following materials were used:

Stellerite rocks were provided by Resources Administration of Ziyuan County, Guangxi province, China. Its degree of whiteness was more than 90% and it was composed of stellerite crystalline, a little of quartz. The composition mainly composed of SiO_2 , Al_2O_3 , CaO , as well as traces of Fe_2O_3 , MgO , etc. The $\text{SiO}_2/\text{Al}_2\text{O}_3$ ratio is about 7. The chemical composition of stellerite rocks is listed in Table 1. $\text{Na}_2\text{SiO}_3 \cdot 9\text{H}_2\text{O}$, NaOH , $\text{Al}(\text{OH})_3$, NaCl , HCl , obtained commercially, were also used for hydrothermal synthesis of zeolites. They were all analytical grade reagent.

Table 1 Chemical composition of stellerite
(mass fraction, %)

SiO_2	Al_2O_3	Si/Al	CaO	K_2O
58. 76	14. 13	3. 529	8. 8	0. 11
Na_2O	Fe_2O_3	H_2O	Volatile	Tatal
0. 18	0. 004	18. 12	17. 79	100. 1

Seed preparation: Solution A was prepared by dissolving $\text{Na}_2\text{SiO}_3 \cdot 9\text{H}_2\text{O}$ into distilled water. Solution B was also prepared by dissolving $\text{Al}(\text{OH})_3$ into concentrated NaOH solution and a diluting step followed. A gel reactant mixture for the synthesis of the

^① [Foundation item] Project ((BK99072)) supported by the Natural Science Foundation of Jiangsu Province, and project (998053301) the Doctoral Foundation of State Education Ministry

[Received date] 200-05-28; [Accepted date] 2001-10-12

zeolite seed was achieved as soon as solution B was slowly dropped into solution A under vigorous stirring. The composition of the mixture was (mol/mol): Na_2O : Al_2O_3 : SiO_2 : H_2O = 13: 1: 10: 320. The mixture was packed into a glass beaker and hydrothermally treated at 373 K for 2 h in an aqueous thermostat. The product was washed, filtered, and dried, until a white powder, the zeolite seed, was obtained.

Zeolite synthesis: Stellerite was grounded in air for 4 h by ball milling and the 85 μm powder was obtained. Then the powder was washed at room temperature for 2 h with HCl solution (100 g stellerite, 8 mL 36% HCl, 330 mL H_2O) followed by filtering and drying. The acid-washed stellerite powder was calcined at 873 K for 4 h inside a muffle to activate the stellerite. The mixture for the synthesis of zeolites was prepared as follows: the activated stellerite, seed, NaCl , and NaOH solution were mixed together to form a homogeneous mixture in which the weight ratio of seed to stellerite was 0.25. The molar proportion of the composition is listed in Table 2. The mixture was sealed into a polytetrafluoroethylene autoclave and placed in constant temperature baking oven and aged at 323 K for 6 h, then treated hydrothermally at 373 K for different duration. The product was washed to $\text{pH} = 9$, and dried to obtain the zeolites. According to the chemical composition of the mixture for the synthesis of zeolites, the samples were divided into four batches: Y1x (sample Y11, Y12, Y13, Y14), Y2x (sample Y21, Y22, Y23, Y24, Y25), Y3x (sample Y31, Y32, Y33, Y34), Y4x (sample Y41, Y42, Y43, Y44, Y45).

X-ray diffraction (XRD) analysis was employed using $\text{Cu}-\text{K}\alpha$ radiation on a Bruker D8 ADVANCE diffractometer. Infrared absorption spectra (FT-IR) of these samples were recorded by Bruker Vector-22 spectrometer.

3 RESULTS AND DISCUSSION

Fig. 1 shows the XRD patterns of zeolite synthesized in hydrothermal system with low $\text{H}_2\text{O}/\text{Na}_2\text{O}$ and higher $\text{Ca}^{2+}/\text{Na}^+$ ratios respectively. From the XRD profile, the dominant crystal phase is P zeolite, and the crystallinity of P zeolite increases with its crystallization time increased from 12 h to 48 h

(Fig. 2). Y Zeolite is hardly observed in this batch. Fig. 3 shows the XRD patterns of zeolites in the second batch Y2x. For all samples Y21 to Y24, the main phase is P zeolite. Although the weak peaks of Y zeolite at $2\theta = 6.4^\circ$ have also detected in the profile, the intensity of Y zeolite increases slowly with crystallization time increasing. The peaks of Y zeolite gradually disappear when the intensity of P zeolite increases. It is observed that the crystallinity of Y zeolite attains its maximal value at point of 36 h by

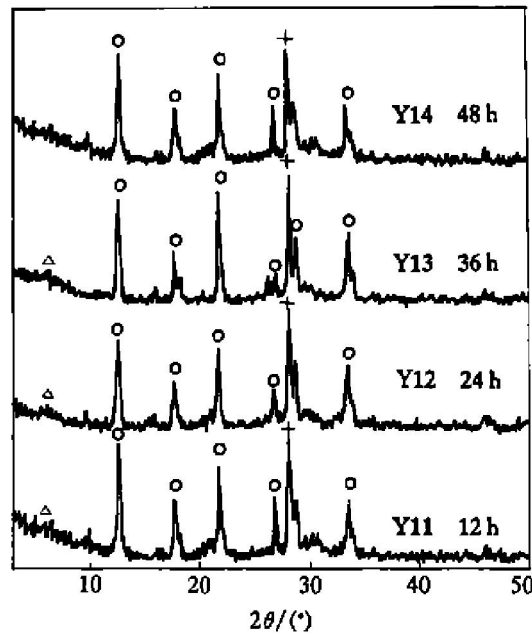


Fig. 1 XRD pattern on samples synthesized under condition of $\text{H}_2\text{O}/\text{Na}_2\text{O} = 30$, $\text{Ca}^{2+}/\text{Na}^+ = 0.16$,
 \triangle —Y zeolite; \circ —P zeolite; $+$ —Quartz

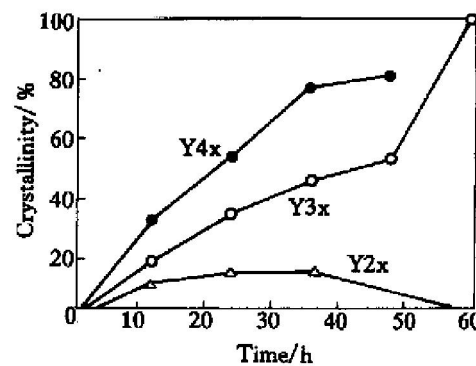


Fig. 2 Relationship between zeolite crystallinity and crystallization time

Table 2 Chemical composition of reaction mixture for Y zeolite (mole fraction, %)

Samples	Na_2O : Al_2O_3 : SiO_2 : H_2O	NaCl	$\text{H}_2\text{O}/\text{Na}_2\text{O}$	$\text{SiO}_2/\text{Al}_2\text{O}_3$	$\text{Ca}^{2+}/\text{Na}^+$
Y21, Y22, Y23, Y24, Y25	2.7: 1: 9: 125	0	46.3	9	0.21
Y31, Y32, Y33, Y34, Y35	2.85: 1: 7: 96.6	10	33.9	7	< 0.16
Y41, Y42, Y43, Y44, Y45	2.85: 1: 7: 96.6	15	33.9	7	< 0.15
Y11, Y12, Y13, Y14	4: 1.4: 10: 120	0	30	7.14	0.16

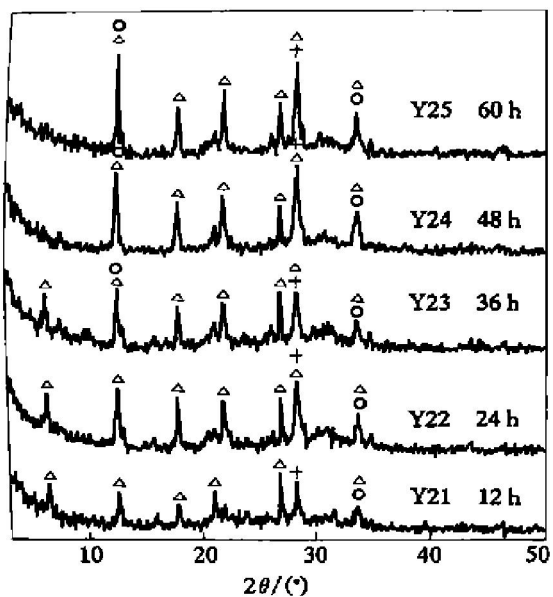


Fig. 3 XRD pattern on samples synthesized under condition of $\text{H}_2\text{O}/\text{Na}_2\text{O} = 46.3$, $\text{Ca}^{2+}/\text{Na}^+ = 0.21$,
 △—Y zeolite; ○—P zeolite, +—Quartz

examining the crystallinity curve in Fig. 2. The crystallization process could be described as follows: the reactant mixture \rightarrow P zeolite + Y zeolite \rightarrow P zeolite. Meanwhile, a strong peak in this XRD profile is showed at $2\theta = 12.8^\circ$, which is caused mainly by P zeolite for the peak in this range is the combination of the maximal unique peak of P zeolite and extremely weak peak of Y zeolite. The peak at $2\theta = 6.4^\circ$ is the maximal unique peak of Y zeolite, and its lattice space in the range is marked as d_0 . It was found that d_0 -value of Y zeolite in the batch decreases with crystallization time increasing. When the XRD analysis data are examined in details, namely, the shifts of d_0 -value are 13.83037 \AA (Y21) \rightarrow 13.73081 \AA (Y22) \rightarrow 13.69625 \AA (Y23) \rightarrow (12.6616 \AA) (Y24) \rightarrow 13.13655 \AA (Y25). Fig. 4 shows the XRD patterns of the samples in the third batch. Here, the $\text{H}_2\text{O}/\text{Na}_2\text{O}$ and $\text{Ca}^{2+}/\text{Na}^+$ ratios are 33.9 and 0.16 respectively. From these patterns it could be found that Y and P zeolite are formed simultaneously after treated hydrothermally for 12 h. After hydrothermal treatment for 24 h, the peaks of P zeolite disappear. The peak intensity of Y zeolite increases with the crystallinity of Y zeolite increasing (Fig. 2). The shifts of d_0 -value in this batch are 14.32437 \AA (Y31) \rightarrow 14.30741 \AA (Y32) \rightarrow 14.29920 \AA (Y33) \rightarrow 14.28428 \AA (Y34). Fig. 5 shows that the crystal phase of all the samples in the fourth batch (Y4x) is only Y zeolite. The crystallinity of Y zeolite increases and the peak of the residual quartz at $2\theta = 28^\circ$ decreases gradually with crystallization time increasing from 12 h to 48 h. The shifts of d_0 -value in the fourth batch are: (14.03359 \AA) (Y41) \rightarrow 14.09332 \AA (Y42) \rightarrow 14.00330 \AA (Y43) \rightarrow

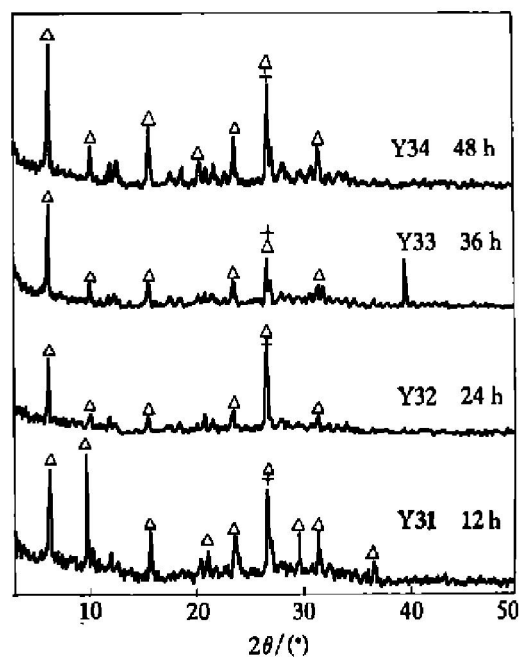


Fig. 4 XRD pattern on samples synthesized under condition of $\text{H}_2\text{O}/\text{Na}_2\text{O} = 33.9$, $\text{Ca}^{2+}/\text{Na}^+ = 0.15$,
 △—Y zeolite, ○—P zeolite, +—Quartz

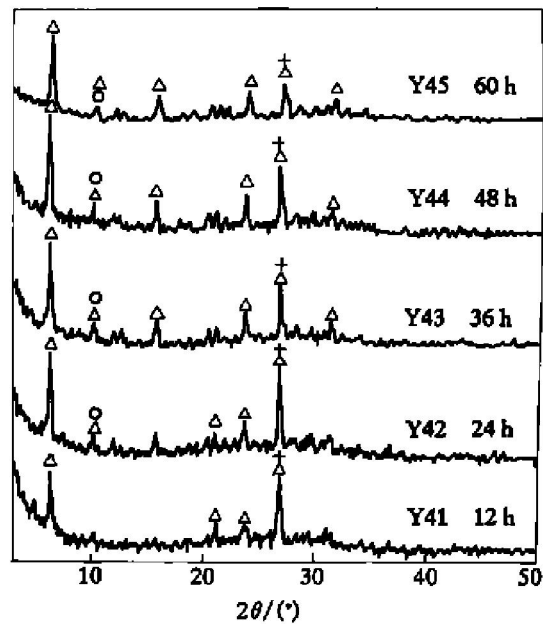


Fig. 5 XRD pattern on samples synthesized under condition of $\text{H}_2\text{O}/\text{Na}_2\text{O} = 33.9$, $\text{Ca}^{2+}/\text{Na}^+ = 0.15$,
 △—Y zeolite, ○—P zeolite, +—Quartz

14.1378561 \AA (Y44). The d_0 -values bracketed are considered as inaccurate measurement due to device or operation.

Comparing the phase transformation of zeolites synthesized under four different hydrothermal conditions, it is apparent that the $\text{H}_2\text{O}/\text{Na}_2\text{O}$ and $\text{Ca}^{2+}/\text{Na}^+$ ratios have great influence on zeolite formation. It is easier to form Y zeolite than P zeolite in hydrothermal system with low $\text{Na}_2\text{O}/\text{H}_2\text{O}$ and low

$\text{Ca}^{2+}/\text{Na}^+$ ratios. The crystallinity of zeolite increases and its lattice space decreases with crystallization time increasing, meanwhile, the $\text{SiO}_2/\text{Al}_2\text{O}_3$ ratio is increased.

Fig. 6 shows the IR spectra of the samples in the first batch ($\text{Y}1x$). It is seen that the intensities and locations of the bands at 432 cm^{-1} , 450 cm^{-1} and 603 cm^{-1} have not changed observably. The bands at 432 cm^{-1} and 450 cm^{-1} are associated with structure-insensitive T-O bonding modes of tetrahedral TO_4 units ($\text{T} = \text{Si}$ or Al)^[8]. The band at 603 cm^{-1} was assigned to structural elements of six-rings^[9, 10] that may act as precursors for the nucleation events. Although the band at 603 cm^{-1} is clearly detected, Y zeolite is not observed by XRD (Fig. 1). These phenomena are attributed to the fact that the growth of Y zeolite is restrained by overwhelming growth of P zeolite in hydrothermal system with higher alkalinity. Bands at $670\text{ cm}^{-1} \sim 700\text{ cm}^{-1}$ and 742 cm^{-1} are associated with inter-bonding vibration of O-Si(Al)-O or O-Si-O . The intensity of the former band increases and it shifts to higher wavenumbers, namely, the shift of the bands is $680\text{ cm}^{-1} \rightarrow 680.7\text{ cm}^{-1} \rightarrow 682.7\text{ cm}^{-1} \rightarrow 690.4\text{ cm}^{-1}$. The bands at $1020\text{ cm}^{-1} \sim 1034.5\text{ cm}^{-1}$ and 970 cm^{-1} which are regarded as antisymmetric stretching of O-Si(Al)-O moved to higher wavenumber ($1020\text{ cm}^{-1} \rightarrow 1023\text{ cm}^{-1} \rightarrow 1032.5\text{ cm}^{-1} \rightarrow 1034.5\text{ cm}^{-1}$) and the intensity also increases with crystallization time increasing. The other bands at 1490 cm^{-1} and 1641.1 cm^{-1} are due to rudimental CaCO_3 in stellerite and adsorbed water^[11]. The IR spectrum of batch $\text{Y}2x$ show (Fig. 7) that the number of IR absorption peaks in the range of $900\text{ cm}^{-1} \sim 400\text{ cm}^{-1}$ increases with crystallization time increasing. The intensity of band around 600 cm^{-1} and the complexity of the spectral

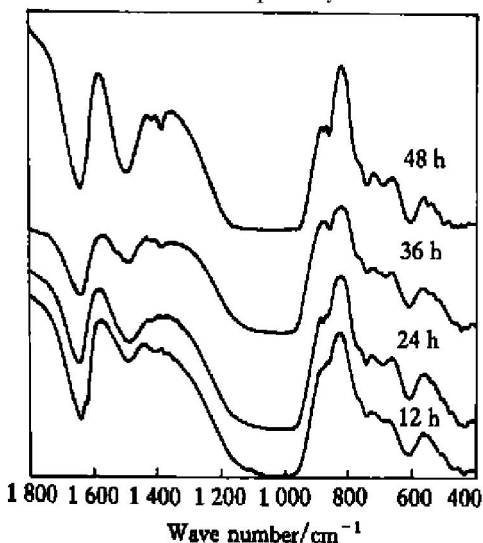


Fig. 6 IR spectrum of samples synthesized under condition of $\text{H}_2\text{O}/\text{Na}_2\text{O} = 30$, $\text{Ca}^{2+}/\text{Na}^+ = 0.16$

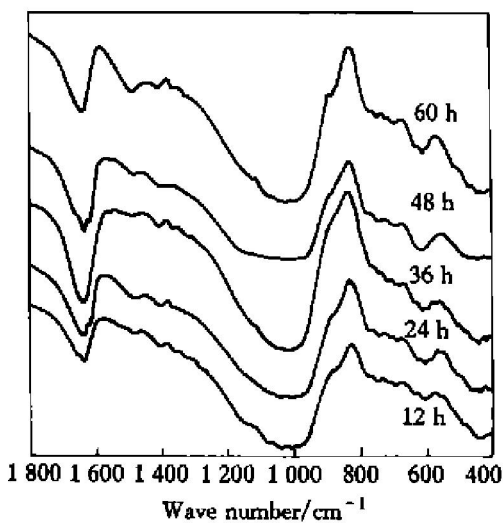


Fig. 7 IR spectrum of samples synthesized under condition of $\text{H}_2\text{O}/\text{Na}_2\text{O} = 46.3$, $\text{Ca}^{2+}/\text{Na}^+ = 0.21$

lines in the range of $900\text{ cm}^{-1} \sim 400\text{ cm}^{-1}$ attains their maxima after hydrothermal treatment for 36 h. The result is uniform that detected by XRD as shown in Figs. 2 and 5. The IR spectral profile is very different between batches $\text{Y}3x$, $\text{Y}4x$ and $\text{Y}1x$, $\text{Y}2x$. Although the number and the shape of IR absorption peaks in batch $\text{Y}3x$ and $\text{Y}4x$ are approximately same under same crystallization time, and the intensities of these peaks in batch $\text{Y}3x$ (Fig. 8) are weaker than that in batch $\text{Y}4x$ (Fig. 9). This difference between $\text{Y}3x$ and $\text{Y}4x$ is caused by different $\text{Ca}^{2+}/\text{Na}^+$ ratio in their hydrothermal system. It is considered that the growth process of Y zeolite is accelerated in hydrothermal system containing higher content of Na^+ . The changes of absorption peaks in batch $\text{Y}4x$ from $\text{Y}41$ to $\text{Y}45$ is as follows: (12 h) 466.7 cm^{-1} , 603.6 cm^{-1} , $864\text{ cm}^{-1} \rightarrow$ (24 h) 462.8 cm^{-1} , 597.8

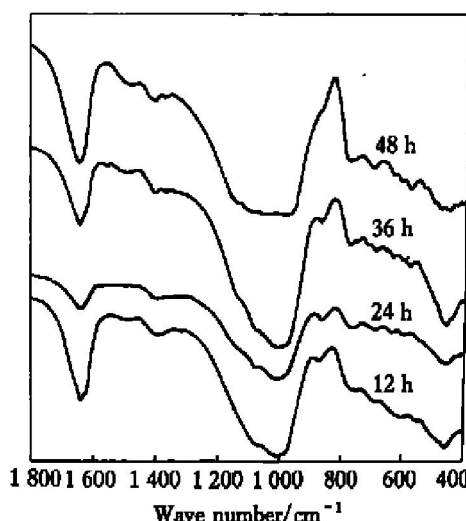


Fig. 8 IR spectrum of samples $\text{Y}3x$ synthesized under condition of $\text{H}_2\text{O}/\text{Na}_2\text{O} = 33.9$, $\text{Ca}^{2+}/\text{Na}^+ = 0.15$

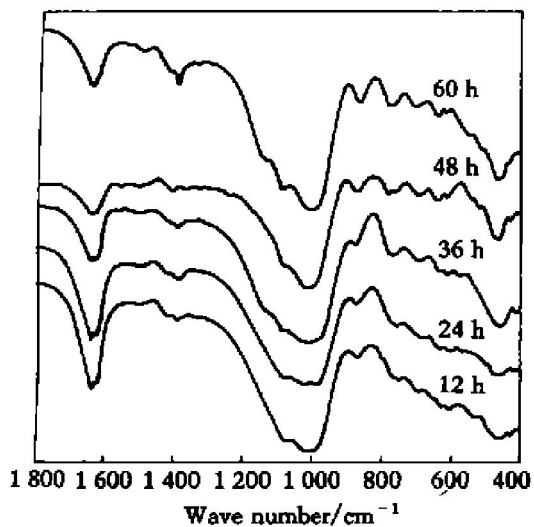


Fig. 9 IR spectrum of samples Y4x synthesized under condition of $\text{H}_2\text{O}/\text{Na}_2\text{O} = 33.9$, $\text{Ca}^{2+}/\text{Na}^+ = 0.15$

cm^{-1} , 628.7 cm^{-1} , 748.2 cm^{-1} , $867.8\text{ cm}^{-1} \rightarrow$ (36 h) 457 cm^{-1} , 607.5 cm^{-1} , 682.7 cm^{-1} , 767.5 cm^{-1} , $867.8\text{ cm}^{-1} \rightarrow$ (48 h) 462.8 cm^{-1} , 603.6 cm^{-1} , 680.7 cm^{-1} , 775.2 cm^{-1} , $864\text{ cm}^{-1} \rightarrow$ (60 h) 460.9 cm^{-1} , 607.5 cm^{-1} , 692.3 cm^{-1} , 771.4 cm^{-1} and 860 cm^{-1} . The appearance of bands at 682.7 cm^{-1} , 767.5 cm^{-1} and the rise of their intensities are related to the formation and crystallinity increasing of Y zeolite. It was verified that the $\text{SiO}_2/\text{Al}_2\text{O}_3$ ratio in zeolites increased as the new bands at 682.7 cm^{-1} and 767.5 cm^{-1} moved to higher wavenumber.

3 CONCLUSIONS

Y and P zeolite were successfully synthesized hydrothermally from natural stellerite. The results showed that the higher crystallinity of Y zeolite can be obtained in hydrothermal system with low alkalinity, low $\text{Ca}^{2+}/\text{Na}^+$ and higher $\text{SiO}_2/\text{Al}_2\text{O}_3$ ratios. The lattice space is decreased with crystallization time increasing. P zeolite is prompted under condition of higher alkalinity and $\text{Ca}^{2+}/\text{Na}^+$ ratio. IR spectrum measurement show that the intensity and number of bands in the range of $400\text{ cm}^{-1} \sim 900\text{ cm}^{-1}$ increase obviously with crystallization time increasing. Bands 680 cm^{-1} , 760 cm^{-1} and 860 cm^{-1} corresponding to

Y zeolite appear during later crystallization stage. Most of these bands move to higher wavenumber, meanwhile, $\text{SiO}_2/\text{Al}_2\text{O}_3$ ratio increases generally. In hydrothermal system with reverse condition above, bands 600 cm^{-1} and $420\text{ cm}^{-1} \sim 470\text{ cm}^{-1}$ hardly change with crystallization time increasing.

[REFERENCES]

- [1] Schmacht M, Kim T J, Gril W, et al. Ultrasonic monitoring of zeolite synthesis in real time [J]. Ultrasonics, 2000, 38: 809– 812.
- [2] Seidel A, Joachim L, Boddenberg B. Copper nanoparticles in Y zeolite [J]. J Mater Chem, 1999, 9: 2495– 2498.
- [3] Van Bokhoven J A, Miller J T, Nachtegaal G H, et al. Changes in structural and electronic properties of the zeolite framework induced by extra-framework Al and La in H-USY and La(x) NaY: A Si and Al MAS NMR and Al MQ MAS NMR study [J]. J Phys Chem B, 2000, 104: 6743– 6754.
- [4] Sasaki Y, Suzuki T, Takamura Y, et al. Structure analysis of the mesopore in dealuminated Y zeolite by higher resolution TEM observation with slow scan CCD camera [J]. J Catalysis, 1998, 178: 94– 100.
- [5] Burriesci N, Crisafulli M, Giodano N, et al. Hydrothermal synthesis of zeolites from low-cost natural silica-alumina sources [J]. Zeolites, 1984, 4: 384– 388.
- [6] Aiello R, Nastro A, Crea F. Use of natural products for zeolite synthesis. V. Self-bonded P zeoliteellets from rhyolitic pumice [J]. Zeolites, 1982, 2: 290– 294.
- [7] Gabriela de la Puente, Eduardo Falvabella Souza Aguiar, Fatima Marla Zanon Zoton, et al. Influence of different rare earth ions on hydrogen transfer over Y zeolite [J]. Applied Catalysis A, General, 2000, 197: 41– 46.
- [8] Wantae Kim, Qiu Zhang, Fumio Saito. Synthesis of zeolite A and X from kaolinite activated by mechanochemical treatment [J]. J Chemical Engineering, (in Japanese), 2000, 33(2): 217– 222.
- [9] Carlos de las Pozas, David Diaz Quintanilla, Joaquin Perez Pariente, et al. Hydrothermal transformation of natural clinoptilolite to zeolites Y and P1: Influence of the Na, K content [J]. Zeolite, 1989, 9: 33– 39.
- [10] Svetlana Mintova, Norman H. Olson, Thomas Bein. Electron microscopy reveals the nucleation mechanism of Y zeolite from precursor colloids [J]. Angew Chem Int Ed, 1999, 38(21): 3201– 3204.
- [11] Takae Kawai, Kazuo Tsutsumi. A study on the surface silanol groups developed by hydrothermal and acid treatment of faujasite type zeolites [J]. Journal Colloid and Interface, 1998, 212: 310– 316.

(Edited by ZHU Zhong-guo)